Kap104p imports the PY-NLS-containing transcription factor Tfg2p into the nucleus

Katherine E. Süel and Yuh Min Chook

Supplemental Data

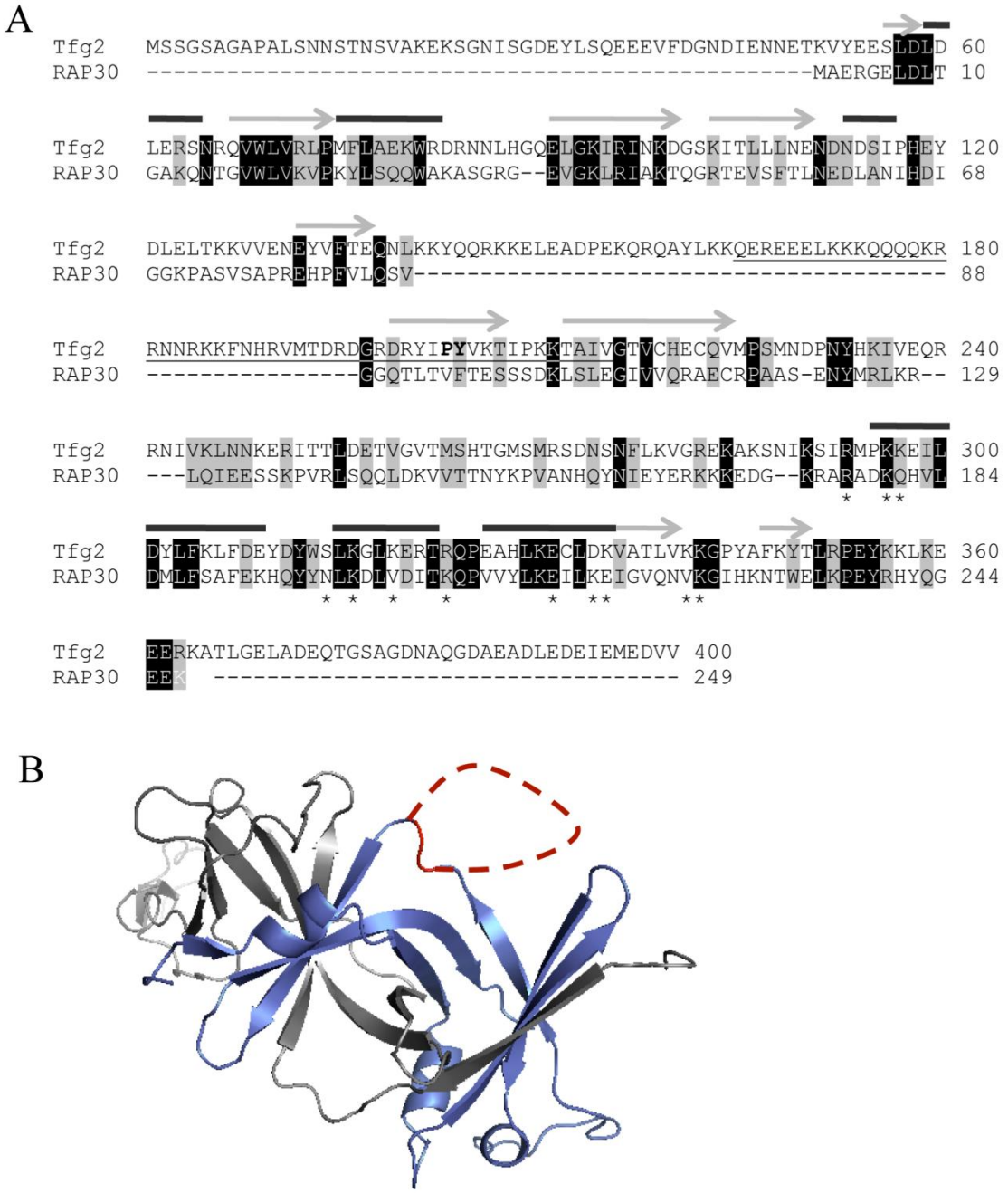

Figure S1. (A) Alignment of *S. cerevisiae* Tfg2p with its human homolog RAP30. The PY-NLS is underlined and the PY motif is in bold. Identical residues are highlighted in black and similar residues in gray. Beta strands are represented by gray arrows and alpha helices by black bars. Secondary structure labels are from the RAP30 crystal (1f3u) and NMR structures (1bby). Asterisks denote residues mutated in the DNA binding domain. (B) Crystal structure of RAP74 (gray)/ RAP30 (blue) homodimerization domains. The PY-NLS insertion (red dashed line) is between RAP30 residues 88 and 89 (red solid line). Figure was made from pdb file 1f3u in PyMOL (*1*, *2*).

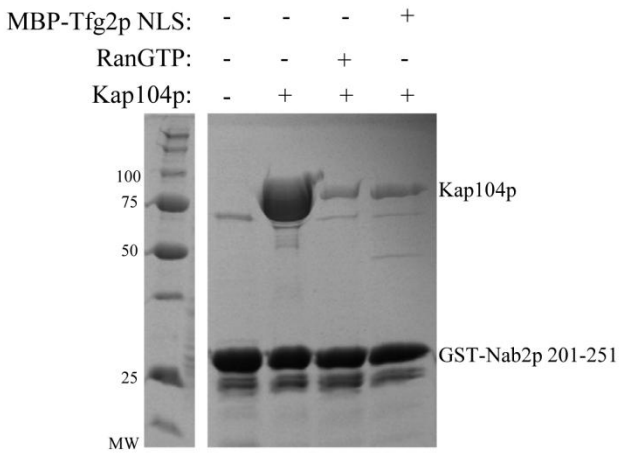

Figure S2. Tfg2p PY-NLS dissociates Kap104p from Nab2p PY-NLS. Kap104p was added to immobilized GST-Nab2p PY-NLS in the absence and presence of RanGTP or MBP-Tfg2p PY-NLS.

A 341 KGPYAFKYTLRPEYKKLKEEERKATLGELADEQ 374

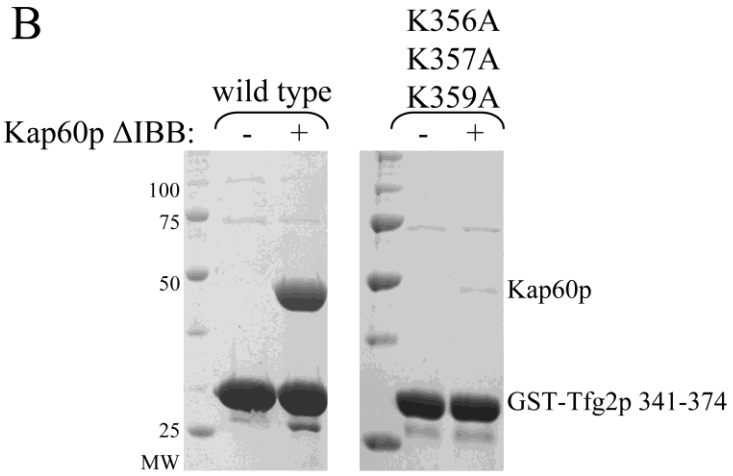

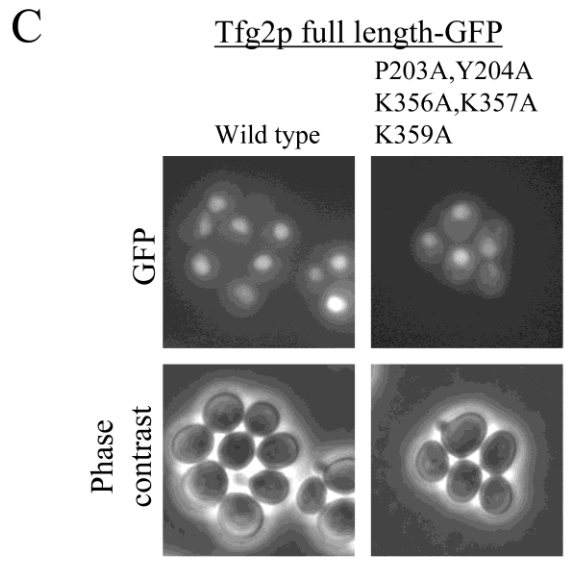

Figure S3. Tfg2p has a non-functional cNLS. A) Sequence of a predicted cNLS in Tfg2p. The cNLS is underlined. B) Kap60p binds the putative NLS and mutagenesis of the cNLS abolished binding. Kap60p was added to immobilized wild type or mutant GST-Tfg2p cNLS. C) The cellular localization of Tfg2p-GFP is not affected by mutations in the PY motif and in the cNLS. Localization in wild type yeast cells were analyzed by fluorescence microscopy and phase contrast.

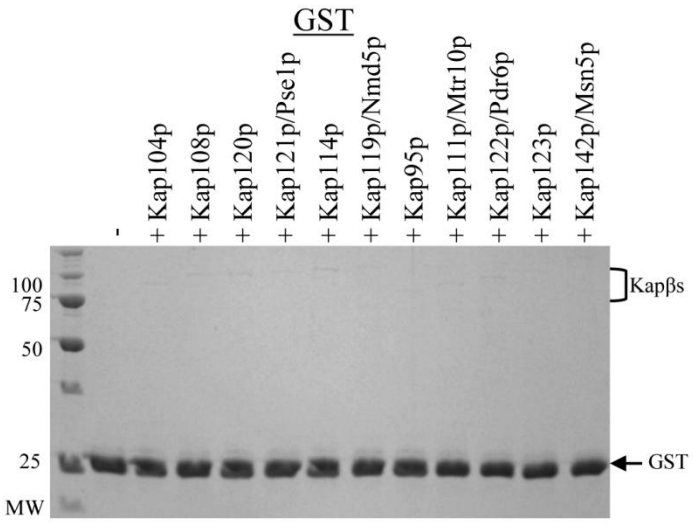

Figure S4. Binding assay of recombinant Kapβs with immobilized GST. Proteins were visualized by Coomassie staining.

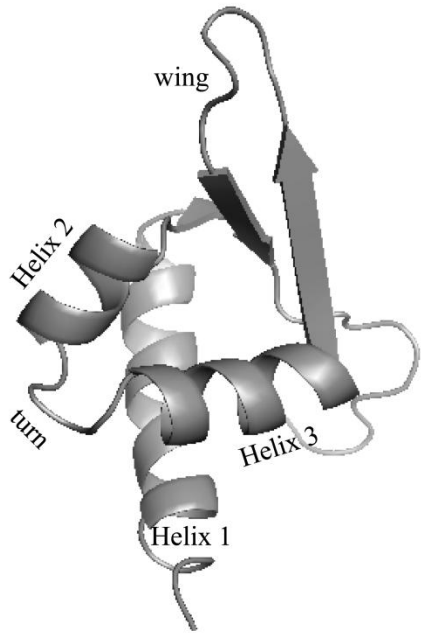

Figure S5. NMR structure of RAP30 DNA binding domain. Figure was made from pdb file 1bby using PyMOL (*2*, *3*).

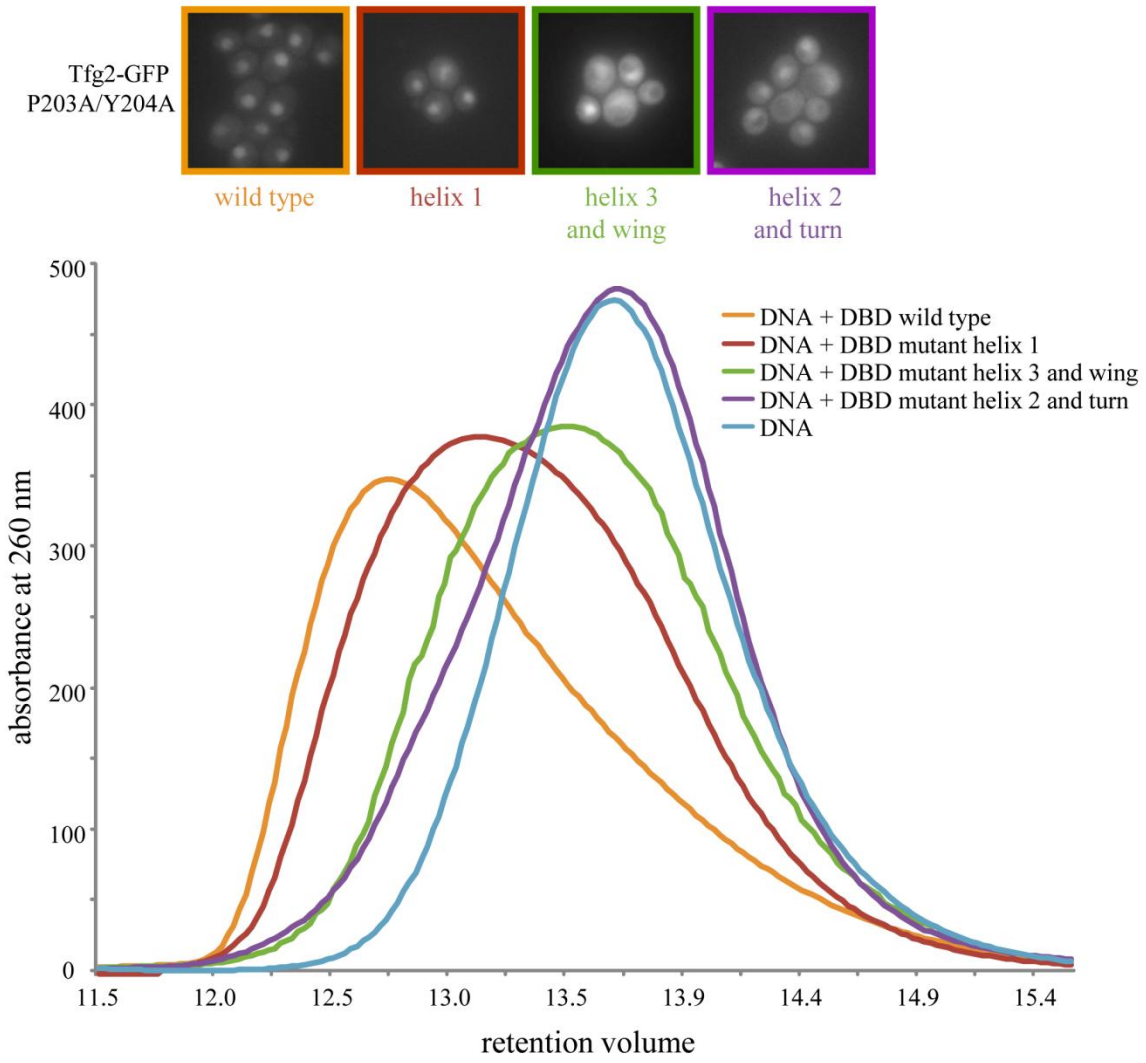

Figure S6. Point mutations in Tfg2p DNA binding domain affect DNA binding. DNA was applied to a size exclusion column in the presence and absence of Tfg2p DBD and its absorbance was monitored at 260 nm. The addition of wild type DBD (orange) shifted the DNA peak (blue), indicating complex formation. DBD with mutations in helix 1 (red) or helix 3 and wing (green) bound DNA, but to a lesser extent than wild type. DBD with mutations in helix 2 and turn (purple) did not cause a shift in the DNA peak indicating that it was unable to bind DNA. The four panels above the chromatogram are wild type yeast cells expressing full length ^{203}PY^{204}/AA mutant Tfg2p-GFP fusion proteins with mutations in the indicated helices of the DNA binding domain.

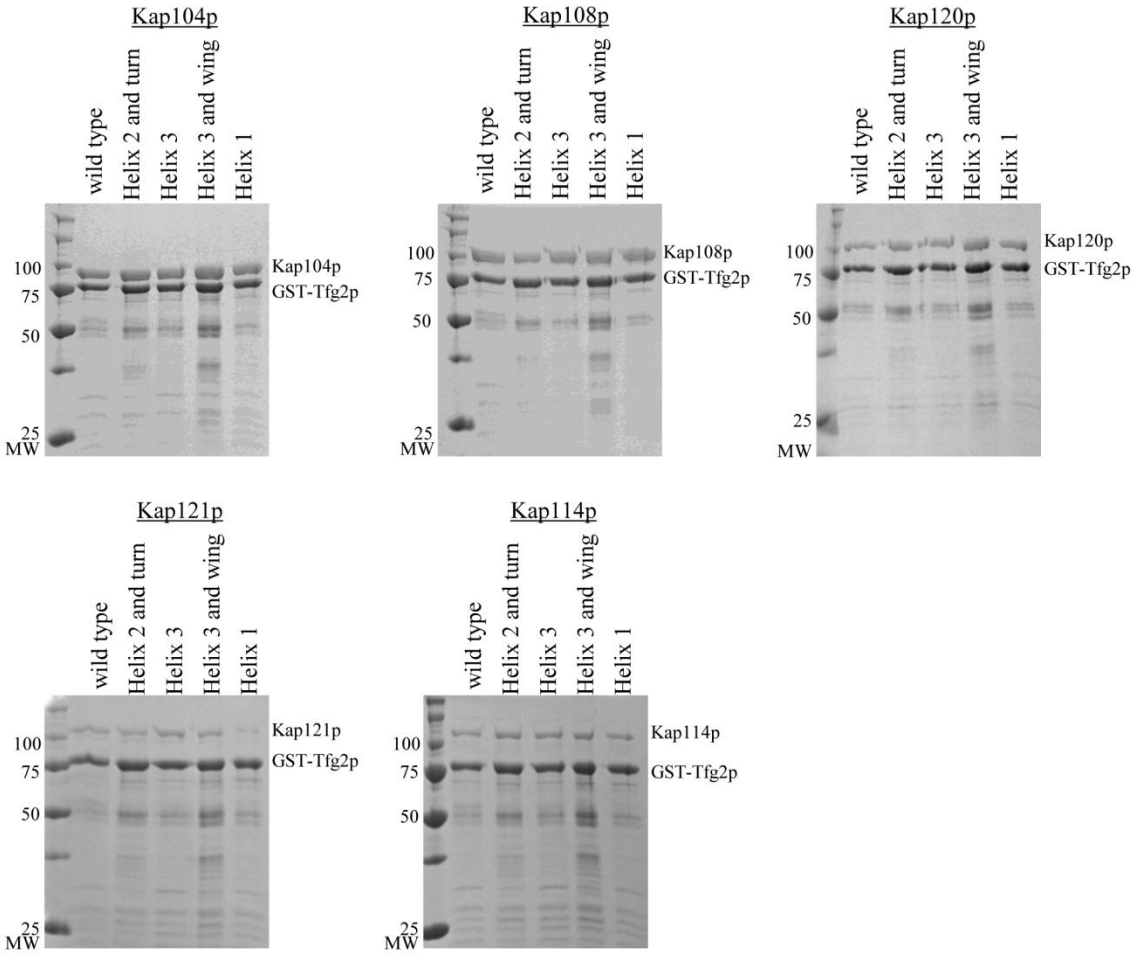

Figure S7. Point mutations in the DNA binding domain do not affect Kapβ interactions. Kap104p, Kap108p, Kap120p, Kap121p, or Kap114p were added to immobilized wild type or mutant GST-full length Tfg2p. Mutants are labeled as in the text and in Figure 6. Proteins were visualized by Coomassie staining.

Supplemental Methods

Cloning, protein expression and purification of Tfg2 DBD-
Tfg2 DBD (284-365) was subcloned from the full length construct into the pGexTev vector. All point mutations were cloned using the QuikChange method (Stratagene) and confirmed by nucleotide sequencing. GST-DBD proteins were expressed and purified using the same method as GST-Kapβ.
Gel filtration chromatography assay-
5.2 nmol HIV-2 promoter DNA (GATATACCCG CTGCTC) (*3*) was subjected to gel filtration chromatography over a Superdex 75 (GE Healthcare) in the presence and absence of wild type and mutant Tfg2p DBD (1:2 DNA:DBD molar ratio). Absorbance was measured at 260 nm.

Supplemental References

1. Gaiser, F., Tan, S., and Richmond, T. J. (2000) Novel dimerization fold of RAP30/RAP74 in human TFIIF at 1.7 A resolution, *J Mol Biol 302*, 1119-1127.
2. DeLano, W. L. (2002) The PyMOL User's Manual, DeLano Scientific, San Carlos, CA
3. Groft, C. M., Uljon, S. N., Wang, R., and Werner, M. H. (1998) Structural homology between the Rap30 DNA-binding domain and linker histone H5: implications for preinitiation complex assembly, *Proc Natl Acad Sci U S A 95*, 9117-9122.